ACCOUNTS
of chemical research

Responsive MRI Agents for Sensing Metabolism *in Vivo*

LUIS M. DE LEON-RODRIGUEZ,[†] ANGELO JOSUE M. LUBAG,[†] CRAIG R. MALLOY,[†,‡,§,⊥] GARY V. MARTINEZ,[||] ROBERT J. GILLIES,[||] AND A. DEAN SHERRY*[,†,‡,¶]

[†]*Advanced Imaging Research Center,* [‡]*Department of Radiology,* [§]*Department of Internal Medicine, University of Texas Southwestern Medical Center, Dallas, Texas 75235,* [⊥]*VA North Texas Health Care System, Dallas, Texas 75216,* [||]*Department of Biochemistry and Molecular Biophysics, Arizona Cancer Center, University of Arizona, Tucson, Arizona, and the H. Lee Moffitt Cancer Center & Research Institute, Tampa, Florida 33612,* [¶]*Department of Chemistry, University of Texas at Dallas, Richardson, Texas 75083*

RECEIVED ON OCTOBER 16, 2008

CONSPECTUS

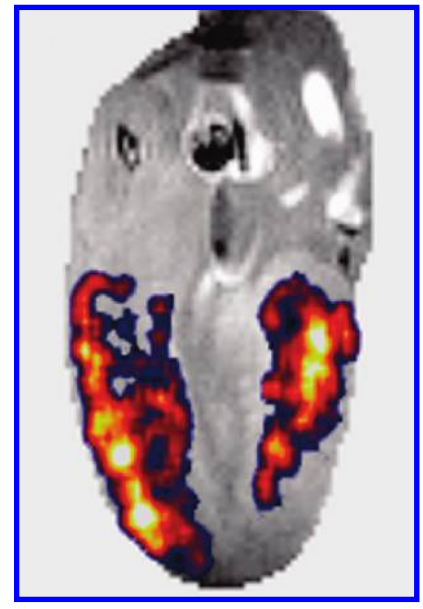

Magnetic resonance imaging (MRI) has inherent advantages in safety, three-dimensional output, and clinical relevance when compared with optical and radiotracer imaging methods. However, MRI contrast agents are inherently less sensitive than agents used in other imaging modalities primarily because MRI agents are detected indirectly by changes in either the water proton relaxation rates (T_1, T_2, and T_2') or water proton intensities (chemical exchange saturation transfer and paramagnetic chemical exchange saturation transfer, CEST and PARACEST). Consequently, the detection limit of an MRI agent is determined by the characteristics of the background water signal; by contrast, optical and radiotracer-based methods permit direct detection of the agent itself. By virtue of responding to background water (which reflects bulk cell properties), however, MRI contrast agents have considerable advantages in "metabolic" imaging, that is, spatially resolving tissue variations in pH, redox state, oxygenation, or metabolite levels. In this Account, we begin by examining sensitivity limits in targeted contrast agents and then address contrast agents that respond to a physiological change; these responsive agents are effective metabolic imaging sensors.

The sensitivity requirements for a metabolic imaging agent are quite different from those for a targeted Gd^{3+}-based T_1 agent (for example, sensing cell receptors). Targeted Gd^{3+} agents must have either an extraordinarily high water proton relaxivity (r_1) or multiple Gd^{3+} complexes clustered together at the target site on a polymer platform or nanoparticle assembly. Metabolic MRI agents differ in that the high relaxivity requirement, although helpful, is eased because these agents respond to bulk properties of tissues rather than low concentrations of a specific biological target. For optimal sensing, metabolic imaging agents should display a large change in relaxivity (Δr_1) in response to the physiological or metabolic parameter of interest.

Metabolic imaging agents have only recently begun to appear in the literature and only a few have been demonstrated *in vivo*. MRI maps of absolute tissue pH have been obtained with Gd^{3+}-based T_1 sensors. The requirement of an independent measure of agent concentration in tissues complicates these experiments, but if qualitative changes in tissue pH are acceptable, then these agents can be quite useful. In this review, we describe examples of imaging extracellular pH in brain tumors, ischemic hearts, and pancreatic islets with Gd^{3+}-based pH sensors and discuss the potential of CEST and PARACEST agents as metabolic imaging sensors.

Published on the Web 03/06/2009 www.pubs.acs.org/acr
10.1021/ar800237f CCC: $71.50

Introduction

Magnetic resonance imaging is a spectacular tool for providing high resolution anatomical imaging of animals and humans but is markedly less sensitive than optical or radiotracer imaging modalities for most molecular imaging applications. Most chemists are familiar with small molecule MRI agents that alter image contrast by changing T_1 or T_2 of water but many may not be aware of the limitations of such agents for molecular imaging *in vivo*. Gd^{3+}-based agents are widely accepted by clinicians because they are easy to administer and provide positive contrast (image brightening) rather than negative contrast (image darkening). Currently available low molecular weight Gd^{3+} chelates distribute into all extracellular space[1−3] and produce tissue brightening in proportion to the extracellular space of each tissue type. A standard clinical injection dose of 0.1 mmol/kg corresponds to an average extracellular tissue concentration of ∼0.5 mM and, given a typical relaxivity of 4 mM^{-1} s^{-1} for a clinical Gd^{3+}-based agent, this corresponds to an increase in water proton relaxation rate of 2 s^{-1}, a value that is easily detected at common imaging fields. Rooney, et al.[4] have demonstrated that extracellular contrast agents are even easier to detect at high magnetic fields due to an increase in T_1 that accompanies moving to higher fields. This suggests that lower doses of contrast agent will be equally effective at higher imaging fields. The detection limit of a targeted Gd^{3+}-based T_1 agent is less easily predicted because local tissue contrast depends upon many factors including the imaging pulse sequence, pixel size, water access to the Gd^{3+} complex at the targeted site, and the relaxivity of the targeted agent *in vivo*.

One motivation for developing new MRI contrast agents is to add agents that have molecular, physiological, or biochemical specificity. Numerous *in vitro* examples of T_1 or T_2 responsive MR agents have been reported, but only a few have been demonstrated *in vivo*. The classic example of a responsive T_1 agent first reported by Moats, Fraser, and Meade[5] was later demonstrated to respond as anticipated after injection into *Xenopus laevis* embryos.[6] Perez et al.[7] also demonstrated the use of small iron oxide particulates as a platform for magnetic resonance T_2 switches; this technology continues to evolve in a number of laboratories.[8−10] Superparamagnetic iron oxide nanoparticles have also been investigated for targeting tumors and tracking stem cells, but these agents typically do not "respond" to their local tissue environment or to physiology and hence have not been used to image metabolism *in vivo*.[11] The goal of this Account is to compare the sensitivity limits and options for T_1 shortening agents for molecular targeting versus responsive agents for monitoring metabolism *in vivo*.

The Detection Limit of Targeted Gd^{3+}-Based T_1 Agents. How Much Does One Need?

If one asked users to approximate the detection limit of a typical Gd^{3+}-based T_1 agent would be, one would likely get widely diverse answers ranging from ∼500 μM to perhaps as low as 50 μM. We recently addressed this question systematically to determine the lower detection limit (DL) of a GdDOTA−peptide capable of targeting to a specific protein. The r_1 relaxivity of this conjugate was 10.7 mM^{-1} s^{-1}, and its estimated DL in solution was 9 ± 3 μM.[12] Upon binding of this Gd^{3+}−peptide conjugate to its target protein on agarose beads, the relaxivity of the agent increased to 17 mM^{-1} s^{-1}, and its DL decreased to 4 ± 1 μM. These experiments allowed us to predict the lower DLs of other molecularly targeted Gd^{3+} complexes, reaching the conclusion that a targeted Gd^{3+} complex with a fully bound relaxivity of 100 mM^{-1} s^{-1} would be detected at 690 nM. A molecular relaxivity of 100 mM^{-1} s^{-1} has proven difficult to achieve using a single Gd^{3+}-polyamino-polycarboxylate complex, but one could easily reach 100 mM^{-1} s^{-1} by multiplexing eight small Gd^{3+} complexes having a relaxivity of 12.5 mM^{-1} s^{-1}. Although a number of novel faster water exchange systems have predicted motionally restricted relaxivities of 100−350 mM^{-1} s^{-1},[13] those systems have not yet been applied *in vivo*, so we chose to test our predictions using rather standard polymeric structures based upon the clinically proven Gd^{3+}-polyamino-polycarboxylate complexes.

To test our DL predictions, a small lysine-based dendron consisting of eight GdDOTA units was prepared, and each Gd^{3+} center had a r_1 of 12.3 ± 0.5 mM^{-1} s^{-1} (37 °C, pH 7, 23 MHz) to yield a molecular relaxivity of 98.4 ± 0.5 mM^{-1} s^{-1}(Figure 1). To provide specificity, the dendron was covalently attached to a dimeric peptoid known to bind with high specificity and affinity to the vascular endothelial growth factor receptor 2 (VEGFR-2),[14] an important target in tumor metastasis. The r_1 of the Gd_8-dendron−peptoid conjugate increased only slightly to 120.8 ± 0.5 mM^{-1} s^{-1} when fully bound to the VEGFR-2 on agarose beads. This indicates that each individual GdDOTA unit has considerable motional freedom when bound to the receptor. With this system in hand, we then tested whether VEGFR-2 receptors could be detected in porcine aortic endothelial cells (PAE/KDR) with 2.5 × 10^5 receptors per cell. This corresponded to a receptor concentra-

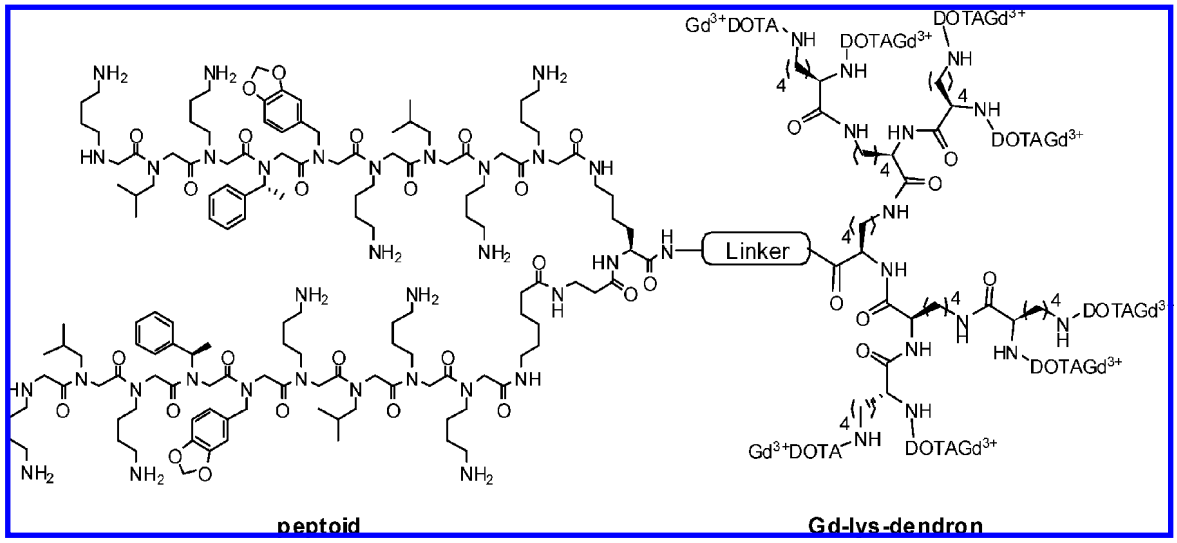

FIGURE 1. A Gd_8-dendron−peptoid used for detection of VEGFR-2 receptors.

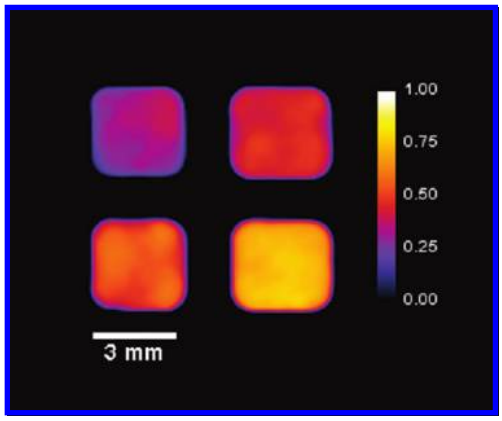

FIGURE 2. Spin−echo T_1-weighted coronal MR images of PBS alone (upper left), 0.5 μM Gd_8-dendron−peptoid agent in PBS (upper right), PAE/KDR cells alone without exposure to the agent (lower left), and PAE/KDR cells exposed to 1 μM agent (lower right). Conditions: 4.7 T; TR = 150 ms; TE = 8.5 ms; FOV = 30 × 30 mm^2; matrix = 128 × 128; avg = 12; 2 mm slice; samples in microtiter wells. A 5 pixel radius median filter was applied to the color image shown (Unpublished).

tion (assuming a cell radius of 5 μm) of about 790 nM, near the DL predicted in ref 12.

PAE/KDR cells were exposed to 1 μM Gd_8-dendron−peptoid in phosphate-buffered saline (PBS) for 30 min at 4 °C followed by imaging. T_1-weighted images of cells exposed to the agent (Figure 2, bottom right) compared with nonexposed control cells (Figure 2, bottom left) were brighter, consistent with agent binding. Given the known binding constant of this targeted agent to the VEGFR2 receptor, one estimates that the local concentration of bound agent in this experiment should be 650 nM. ICP-MS analysis of Gd^{3+} in the pelleted cells gave a measured value of ~700 nM, in agreement with the known receptor concentration. It is clear however that this very low submicromolar concentration in cell receptors is easily detected by MRI as predicted by theory using a relatively simple agent with a molecular relaxivity of only 120 mM^{-1} s^{-1}.

Gd^{3+} Agents That Respond to Tissue Biochemistry: Metabolic Imaging Agents

Our long-term interest in developing MR methods to monitor tissue metabolism *in vivo* has led us to think about the design of contrast agents that respond to important metabolic indices such as tissue pH, tissue redox, hypoxia, and metabolite levels. How do the requirements differ for these applications in comparison to those described above for antigen-targeted Gd^{3+}-based T_1 agents? First, biological indices such as pH, redox, and pO_2 are a bulk property of tissue so the requirement of high relaxivity is not as important here. More important is the *change* in relaxivity (Δr_1) that occurs in response to the metabolic parameter one wishes to monitor by MRI. For example, pH is an important index of metabolism in tissues because excess acid is a hallmark of abnormal metabolism in ischemic tissues, in certain secretory cells, and is certainly important in tumor growth and metastases. Numerous basic publications have reported different designs for pH-sensitive Gd^{3+}-based T_1 agents,[15] but only a few of these have been applied *in vivo*. We will limit our discussions here to those few examples.

The T_1 relaxivity of a Gd^{3+} complex is primarily determined by three factors: q, the number of water molecules in the inner coordination sphere of Gd^{3+}, τ_M, the residence lifetime of these inner-sphere water molecules (how fast they exchange with other water molecules), and τ_R, the rotational correlation time of the agent (how fast the complex tumbles in solution). To prepare a Gd^{3+}-based pH sensor, one only requires a chemical system wherein one or more of these variables (q,

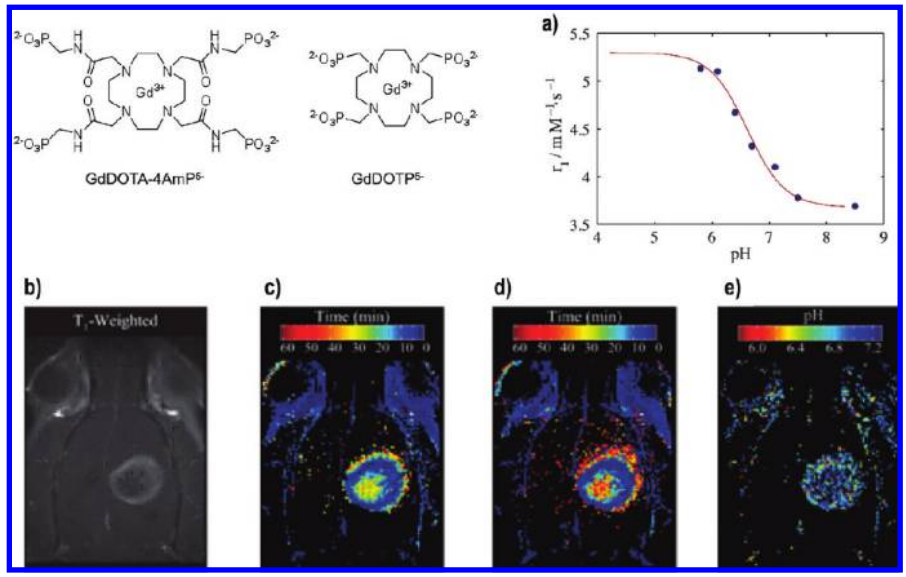

FIGURE 3. Representative time-to-maximal intensity (TMI) images and the calculated pH_e map of a C6 glioma in the brain of a live rat: (a) *in vitro* measurement of r_1 as a function of pH for GdDOTA−4AmP^{5-}; (b) T_1-weighted image of the brain prior to administration of either agent; (c) TMI image after administration of the non-pH-sensitive agent, GdDOTP^{5-}; (d) TMI image after administration of the pH-sensitive agent, GdDOTA−4AmP^{5-}; (e) the resulting calculated pH_e image. Reprinted with permission from John Wiley & Sons, Inc., ref 23, copyright 2006.

τ_M, or τ_R) changes with pH. Examples of all three types can be found in the literature.[16−18] However, the only design that has ever been applied in tissues (perfused tissues or organs or *in vivo*) is GdDOTA−4AmP^{5-} (see structure in Figure 3), an agent that responds to pH by changes in proton exchange (variable τ_M). This agent is unusual because the single inner-sphere water molecule is actually exchanging quite slowly in this complex ($\tau_M = 26\ \mu s$) compared with typical clinical Gd^{3+} agents (τ_M is typically ∼100−200 ns). However, this complex has four appended phosphonate groups that have pK_a's in the range 6.5 to 8, and as these phosphonate groups become protonated below pH ≈ 8, the monoprotonated phosphonate groups hydrogen bond with the single Gd^{3+}-bound water molecule and catalytically exchange the highly relaxed bound water protons with protons of bulk water.[19] This has the same effect as an increase in water exchange rate at the lower pH values even though the actual rate of water molecule exchange is not affected by changes in pH in this complex. Although this represents a rather unusual mechanism for Gd^{3+}-based pH sensor, it should not be surprising that this acid−base catalytic system works so well *in vivo* because acid−base catalysis is a hallmark of many common enzymatic mechanisms in biochemistry.

A major obstacle in applying such systems to image tissue pH is the unknown concentration of the agent in tissue. The measured T_1 contrast of course depends upon two factors, the tissue concentration and the r_1 relaxivity (the pH-dependent parameter). Given that one cannot assume the agent concentration is uniform throughout all tissues and furthermore may be changing with time, any measure of absolute pH requires a correction for any gradient in agent concentration at the moment the image is collected. Aime et al.[20] have pointed out that the ratio, R_{2p}/R_{1p}, of water protons becomes independent of Gd^{3+} concentration for a motionally restricted agent ($\tau_R > 1$ ns) but remains dependent on τ_M, τ_R, and other magnetic parameters that normally affect relaxation in these complexes. They validated the method by demonstrating that the R_{1p} of aqueous samples containing $(GdDOTA)_{33}$−poly-L-ornithine was sensitive to pH due to a conversion of the poly-L-ornithine from a random structure at high pH values to a more ordered helical structure at lower pH values while R_{2p} remains independent of pH. Thus, the R_{2p}/R_{1p} ratio is independent of agent concentration (at least at concentrations high enough to affect these parameters) but is also sensitive to pH, the parameter of interest. While this method is intriguing, the sensitivity of R_{2p}/R_{1p} to change in pH is relatively small, and this may make it difficult to apply *in vivo*.

We have taken a somewhat different approach to image tissue pH by using two Gd^{3+}-based agents with similar chemical characteristics (size and charge), one with a pH-independent and another with a pH-dependent relaxivity. The chemical structures of two such compounds are shown in Figure 3. The r_1 relaxivity of GdDOTP^{5-} is insensitive to changes in pH over a wide range, while the r_1 relaxivity of GdDOTA−4AmP^{5-} changes a modest amount, from 3.5 mM^{-1} s^{-1} at pH 9.5 to 5.3 mM^{-1} s^{-1} at pH 6.3 (see Figures 3 and

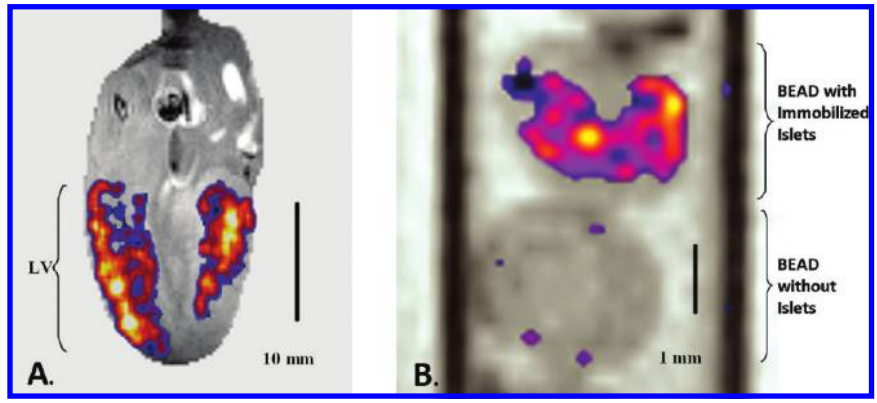

FIGURE 4. (A) MR image of a KCl-arrested rat heart during perfusion with 100 μM GdDOTA−4AmP^{5-}; the gray scale image shows a single slice through the left ventricular wall, while the color overlay reflects the left ventricular muscle regions that became acidic during a 15 min period of global ischemia. (B) MR image of alginate beads containing encapsulated rat pancreatic islets (upper bead; 5% v/v cell-to-bead loading) or empty (lower) perfused with 50 μM GdDOTA−4AmP^{5-}; in this case, the color overlay shows only those voxels where the signal increased above noise after the glucose concentration in the perfusate was increased from 5 to 25 mM. Yellow in the fire-scale color overlays reflects the more acidic regions while purple the less acidic regions. (Unpublished).

5). T_1-weighted dynamic contrast enhanced (DCE) images collected after a bolus injection of one agent followed by images collected after a bolus injection of the second agent provided the data needed to map tissue pH. By making the assumption that the two compounds have identical pharmacokinetics and tissue biodistributions, one can use the image intensity differences at the maximum in the DCE curves to estimate tissue pH. This "dual injection method" has been used to map extracellular tissue pH (pH_e) in mouse kidney[21,22] and in a rat brain glioma (Figure 3).[23] In the glioma model, an intriguing insight provided by the dual injection method includes observation of an inverse relationship between the time-to-maximal intensity (TMI) and pH_e (Figure 3). This indicates that observation of a larger TMI, indicative of slower perfusion in that tumor, was correlated with lower pH_e values.

Although this method works quite well *in vivo*, there are some drawbacks to the successive injection of two different agents. During the course of the injections, prolonged exposure to anesthesia may alter the blood pressure, which can result in significant differences in the TMI in the two injections.[23] In addition, there is a temporal price to pay for two injections because it is necessary to wait until most of the first agent has exited the tumor before administering the second. These considerations make a case for the development of single injection method to enhance the clinical utility of a pH_e sensitive contrast agent.

In many cases, it may not be necessary to measure absolute tissue pH to obtain diagnostically useful information. For example, if the goal is to detect abnormal pH regions of tissues, one might be able to expose the tissue to a pH sensor at a low enough concentration such that significant contrast effects are detected only if tissue pH is abnormally low

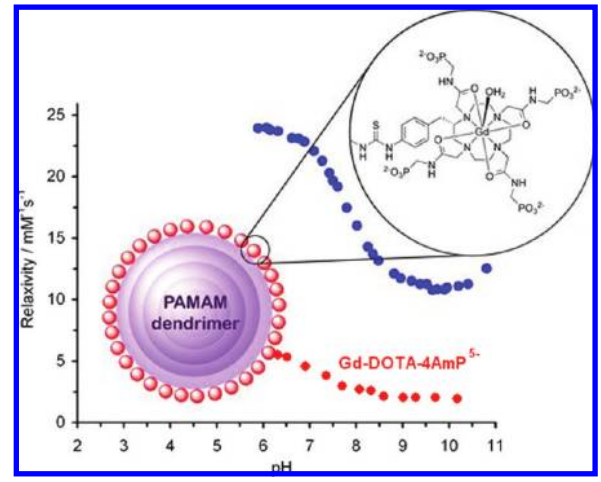

FIGURE 5. T_1 relaxivity versus pH profiles for GdDOTA−4AmP^{5-} and a generation-5 PAMAM dendrimer containing 96 molecules of GdDOTA−4AmP^{5-} attached to its surface. Reprinted with permission from Wiley-VCH Publishers, ref 19, copyright 2008.

(assuming the relaxivity increases at lower pH values as with GdDOTA−4AmP^{5-}). Some disease processes such as malignancies may produce local increases in both extracellular volume and H^+ concentration perhaps improving the threshold for early detection of a cancer or metastasis with water soluble, low molecular weight agents. To illustrate the simplicity of the method, we exposed two different perfused tissue preparations, rat hearts and pancreatic islets, to GdDOTA−4AmP^{5-} and collected T_1-weighted images (Figure 4A). Normoxic hearts perfused with 100 μM agent showed little to no contrast changes after addition of the agent, while ischemic hearts showed regions of brightness, which we attribute to regions of lower pH in ischemic regions generated during the hypoxic period. Similarly, rat islets embedded in agarose beads and perfused with 50 μM GdDOTA−4AmP^{5-} showed little T_1

enhancement until the islets were exposed to high concentrations of glucose to promote glucose-stimulated insulin secretion. Export of insulin from islets is known to be accompanied by release of protons and Zn^{2+} ions from insulin granules. This local increase in proton concentration was easily detected as a change in T_1 after exposure of islets to glucose (Figure 4B). This relatively simple technology offers the opportunity to develop functional assays of islet biology *in vivo*.

Clearly, this simplified approach would work even better if Δr_1, the difference in r_1 between physiological pH and more acidic pH values, was even larger than that displayed by GdDOTA−4AmP^{5-}. Standard theory predicts that the r_1 of a Gd^{3+} complex undergoing fast water exchange will increase upon slowing molecular rotation or tumbling of the molecule in solution (increasing τ_R). However, GdDOTA−4AmP^{5-} is a bit unusual in this context because it has a slowly exchanging water molecule at high pH and a catalytically enhanced proton exchange rate at lower pH values. Based on simple theory, one would predict that the r_1 of the low pH species may become more magnified upon slowing molecular rotation than the r_1 of the slow water exchange species at higher pH. If correct, then Δr_1 could be significantly better for a motionally restricted version of GdDOTA−4AmP^{5-}. To test this, a bifunctional derivative of GdDOTA−4AmP^{5-} was synthesized and reacted with a generation five G5-PAMAM dendrimer having 128 surface amino groups. The product contained on average 96 molecules of GdDOTA−4AmP^{5-} on the surface of the dendrimer with an average hydrodynamic volume consistent with a molecular weight of ∼140 kD.[19] As anticipated, the r_1 of the resulting macromolecular sensor remained pH sensitive (Figure 5) with r_1 increasing from 10.8 mM^{-1} s^{-1} per Gd^{3+} at pH 9.5 to 24.0 mM^{-1} s^{-1} per Gd^{3+} at pH 6. On a macromolecular basis, this corresponds to a change in r_1 from 1037 mM^{-1} s^{-1} at pH 9.5 to 2304 mM^{-1} s^{-1} at pH 6. Thus, Δr_1 for the dendrimer increased 2.2-fold over this pH range in comparison to a Δr_1 of 1.5-fold for monomeric sensor over an identical pH range. It should be pointed out that the mobility of the dendrimer itself is known to be pH-dependent,[24] so part of the change in relaxivity observed in this system may be due to pH-dependent changes in molecular motion of the dendrimer itself and may not solely reflect the pH sensor attached to its surface. Nevertheless, these data show that one could use significantly less pH-sensitive dendrimer (∼0.1−0.3 μM) to detect similar changes in pH by MRI as those demonstrated in Figure 4. This experiment has not yet been performed *in vivo*.

Chemical Exchange Saturation Transfer (CEST) Agents

What other methods might be used to image abnormal pH regions in tissues *in vivo*? Ward et al. were first to demonstrate that image contrast can be altered by taking advantage of chemical species that exchange protons with bulk water via a chemical exchange saturation transfer (CEST) mechanism.[25] Typically, −NH protons in molecules are known to exchange more slowly at low pH than at high pH due to base catalysis of proton exchange, so if the rate of exchange, k_{ex}, is comparable to the chemical shift difference between the exchanging proton and bulk water ($\Delta\omega$), then application of a frequency-selective presaturation pulse at the chemical exchange site prior to collection of an image will result in chemical transfer of some saturated spins into the water pool, thereby reducing the total amount of water detected in the imaging experiment. The amount of chemically transferred spins of course depends upon several factors including k_{ex}, the bulk water T_1, the applied $\mathbf{B}_1$ power, and the concentration of CEST agent.[26,27] These features make CEST agents unique among the MRI contrast agents because contrast is generated only when a presaturation pulse is applied at the frequency of the chemical exchange site. This means that image contrast may be manipulated by the operator! To obtain a CEST image, one collects two images, one after presaturation at the exchange site of interest and another at an equivalent frequency offset on the opposite side of bulk water. The difference between these two image intensities reports the effects of the exchanging CEST species.

A classic example of pH-dependent −NH proton exchange and its relationship to CEST imaging is given by the work of McMahon, et al.,[28] summarized in Figure 6. These data illustrate the influence of an increased rate of −NH proton exchange catalyzed by base on the high-resolution ^{1}H NMR spectrum of poly(L-lysine) (left) and the corresponding Z-spectra or CEST spectra (right). At pH 6, −NH proton exchange is rather slow (50 s^{-1}), and this results in a sharp −NH proton resonance but a rather small CEST effect (top curve in right panel), but at pH 7.9 where −NH proton exchange was increased to 1250 s^{-1}, the high-resolution ^{1}H resonance broadens and almost disappears into the baseline, while CEST is larger (bottom curve in the right panel). This trend would continue at even higher pH values until exchange becomes too fast ($k_{ex} \gg \Delta\omega$) and the CEST effect would once again disappear. This pH dependent effect then becomes the basis of using endogenous proteins that have a large number and vari-

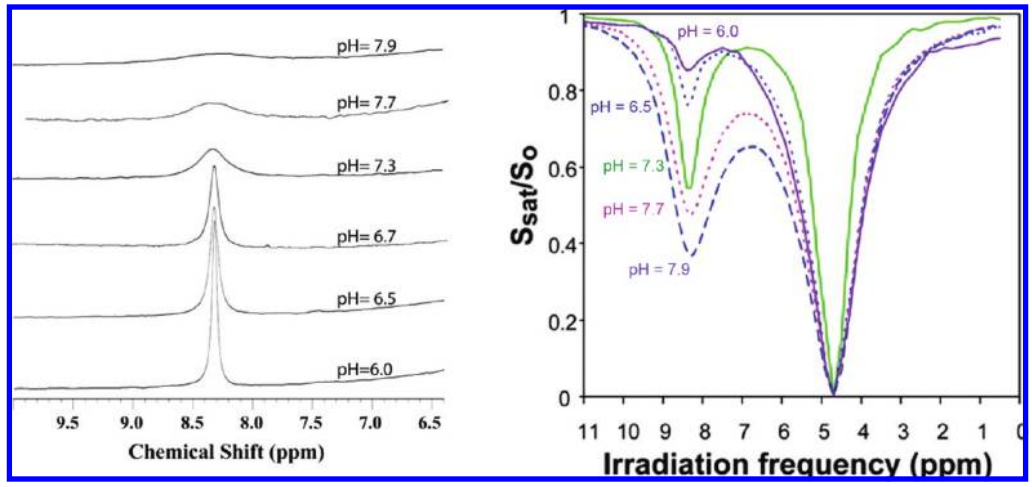

FIGURE 6. High-resolution ^{1}H NMR spectra of the amide protons of poly(L-lysine) as a function of solution pH (left) and the corresponding CEST spectra (right). Reprinted with permission from John Wiley & Sons, Inc., ref 28, copyright 2006.

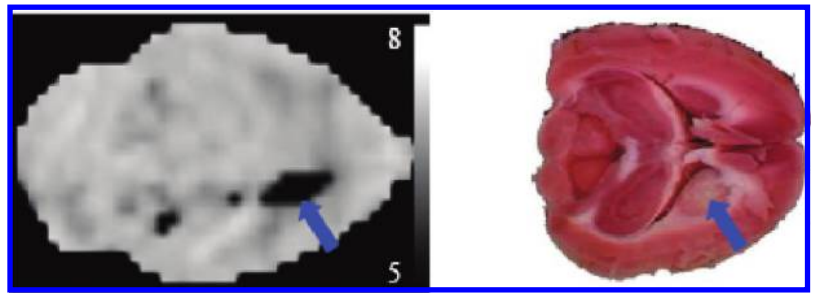

FIGURE 7. An absolute pH map (left) and the corresponding tissue slice of ischemic rat brain stained with 2,3,5-triphenyltetrazolium chloride. The area of infarction visible on the right side of both images corresponds to the caudate nucleus (blue arrow), a region commonly affected by infarction following MCA occlusion. Reprinted with permission from Macmillan Publishers Ltd., ref 29, copyright 2003.

ety of different −NH protons to detect changes in tissue pH by CEST imaging.

The first published example of using protein −NH exchange groups as an endogenous CEST reporter was given by the work of Zhou, et al.[29] Given that the difference in chemical shift between the endogenous −NH proton resonances and bulk water ($\Delta\omega$) is relatively small (on the order of 3 ppm) and the water proton line width *in vivo* is considerably broader than that seen in Figure 6, it becomes necessary to perform an asymmetry analysis to separate out the proton chemical exchange effects from the effects of indirect saturation of water itself.[30] Such analyses are further complicated by the magnetization transfer (MT) effects characteristic of tissues whereby dipolar interactions between water molecules associated with semisolid macromolecules lead to a broad underlying resonance beneath the bulk water resonance. Given the assumption that the contribution of tissue MT is symmetric about the water resonance, collection of two images with a presaturation pulse applied at equal offset frequencies on each side of the bulk water resonance should, in principle, cancel out the MT contribution plus any contribution due to indirect saturation of water itself, leaving only the effects due to CEST. Even though these combined effects can be substantial, Zhou et al.[29] were able to detect ischemic regions in brain where the pH was substantially lower than in the surrounding tissues (Figure 7). In this case, the ischemic region is dark because −NH exchange from endogenous proteins is too slow to detect a CEST effect in those regions where the pH is below 6 or so while the surrounding healthier tissues have a CEST contribution due to −NH proton exchange. The corresponding histological tissue stain confirmed the result reported by CEST imaging.

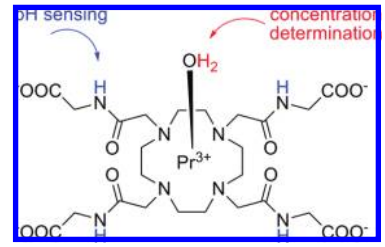

FIGURE 8. PrDOTA−(gly)$_4$: a CEST pH sensor with a built-in concentration indicator.

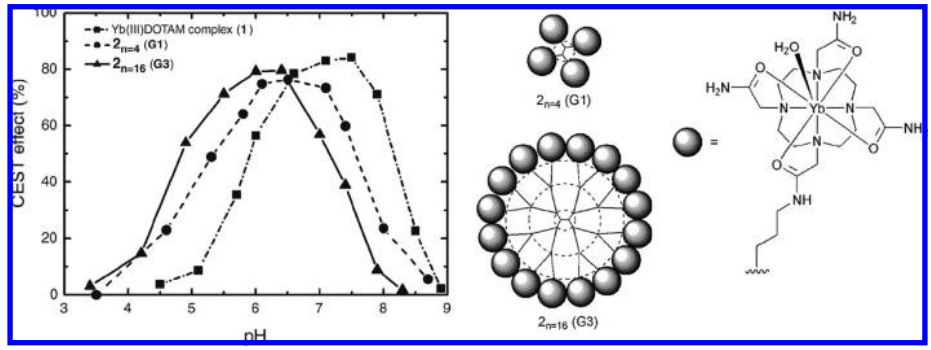

FIGURE 9. Conjugation of the simple tetraamide complex, YbDOTAM, to dendrimers of various size and generation results in −NH proton exchange-based CEST agents with differing pH sensitivities. Reprinted with permission from John Wiley & Sons, Inc., ref 34, copyright 2007.

The paramagnetic lanthanide ions (other than Gd^{3+}) complexed by ligands with exchangeable protons also hold promise as exogenous CEST agents. Given the remarkable hyperfine shifting capabilities of the paramagnetic lanthanide ions, proton (−NH or −OH) or water molecule exchange sites in these complexes are typically frequency-shifted well away from the bulk water resonance ($\Delta\omega$) thereby making direct saturation at those sites considerably more distinct than activation of CEST exchange sites near the bulk water frequency. The resulting PARACEST agents have another advantage in that exchange can be faster while maintaining the intermediate-to-slow exchange condition required for CEST, $\Delta\omega \approx k_{ex}$. These agents have not been used to measure pH *in vivo* at this point, but they do hold promise for nontraditional objectives such as tomographic temperature[31] and glucose imaging.[32,33] Temperature imaging has numerous applications in medicine and physiology because of the fundamental interactions among heat production, metabolism, blood flow, and inflammation, and glucose imaging would be highly relevant to studies of nutrition and diabetes. As pH sensors, PARACEST agents do offer potential advantages over Gd^{3+}-based agents that require infusion of two compounds to correct for any concentration differences. One approach[26] is to build into the same molecule two exchange sites, one insensitive to pH and another sensitive to pH. This was illustrated by the agent PrDOTA−$(gly)_4^-$ (Figure 8), a complex where water exchange is independent of pH (except at the extremes of high and low pH), while CEST from the −NH protons displays a similar pH responsive profile as with other diamagnetic amide −NH protons. In principle then, a pH map of tissues could be obtained after infusion of the single agent followed by CEST measurements using two different presaturation frequencies, the ratio of which would be a direct readout of pH. This agent has not yet been tested *in vivo*.

A third generation G3-dendrimer conjugated with 16 copies of YbDOTAM to increase the sensitivity of CEST was also recently reported (Figure 9).[34] This yielded a molecular system with 48 exchangeable −NH protons that reduced the CEST detection limit into the range of 20 μM, a considerable improvement over simple PARACEST monomers such as that shown in Figure 9. Interestingly, the pH profile of the −NH exchanging protons differed between the monomer, a G1 dendrimer, and the G4 dendrimer, thereby allowing fine-tuning of the pH-sensitive region over which the agent would be responsive. Additionally, a CEST agent concentration independent method for metabolite determination consisting of applying two different radio frequencies for presaturation has also been reported and proven to work *in vitro* for pH mapping using the dendrimer system.[35] This latter approach might provide the pathway for exogenous CEST agents to reach *in vivo* applications.

Summary and Outlook

Responsive MRI agents for monitoring metabolism *in vivo* have only recently begun to appear in the literature, and only a few have been demonstrated *in vivo*. MRI maps of absolute tissue pH can be obtained by using Gd^{3+}-based T_1 agents but the experiments are complicated by the requirement of an independent measure of agent concentration in tissues. Various approaches can be taken to simplify the experimental protocol for obtaining an absolute measure of tissue pH, but if one is simply willing to accept detection of low pH regions in tissue, then these agents can be quite useful. pH sensors based on CEST are in many ways more versatile because exchange sites can be built into molecules to make them concentration independent. Unfortunately, these have yet to be applied *in vivo*. The opportunities to apply clever chemistry to create novel metabolic imaging agents are vast, but chemists should be encouraged to go beyond simply reporting *in vitro* examples and establish long-term collaborations with physiologists and imaging experts to see that such agents get applied *in vivo*. We have held a long-term goal of develop-

ing a simple MR imaging method to monitor pH in tumors, ischemic heart tissues, and islet function in the clinical setting and encourage other investigators to bring new ideas to the table.

We wish to thank the NIH (Grants CA-115531, CA-126608, DK-058398, RR-02584, and EB-04582) and the Robert A. Welch Foundation (Grant AT-584) for partial support of this work.

BIOGRAPHICAL INFORMATION

Luis M. De Leon-Rodriguez received his B.S. in Chemistry in 1996 from the University of Guanajuato and his Ph.D. in chemistry in 2001 from The University of Texas at Dallas. He is a Professor in University of Guanajuato and is currently an Assistant Instructor in the Advanced Imaging Research Center of the UT Southwestern Medical Center. His research interests focus on the synthesis of biospecific agents for molecular imaging.

Angelo Josue M. Lubag received his B.S. and M.S. degrees in Chemistry and Agricultural Chemistry/Biochemistry from the University of the Philippines and his Ph.D. from the University of Texas at Dallas in 2005. He is currently a Postdoctoral Research Fellow at the Advanced Imaging Research Center of the UT Southwestern Medical Center working on MR imaging of metabolic and molecular events in cells, tissues and animals.

Craig R. Malloy received a B.S. in Chemistry from Stanford University and a M.D. from the University of California at San Francisco. He is currently Professor of Internal Medicine and Radiology at the University of Texas Southwestern Medical Center and staff physician at the VA North Texas Health Care System. His research interests include high-field MR imaging and spectroscopy, hyperpolarization, and analysis of metabolic pathways *in vivo*.

Gary Martinez is a senior staff imaging scientist at Moffitt Cancer Center and Research Institute. He received his Ph.D. at the University of California in Santa Cruz under the supervision of Glenn Millhauser (Chemistry). He joined the research group of Robert Gillies in Arizona after a postdoctoral appointment with Prof. S. Wijmenga (Sweden) and NIH NRSA research fellowship with Michael Brown (Arizona). His research interests include *in vivo* pH measurement with MR and methodological advances in cancer detection, prognosis, and therapy response.

Robert J. Gillies received his B.S. in biology in 1974 from UC Irvine and his Ph.D. in 1979 from the University of California, Davis. He had a postdoctoral traineeship with Prof. Robert G. Shulman at Yale University, followed by faculty positions in biochemistry at Colorado State University (1982−1988) and the University of Arizona (1988−2008). He is currently vice chair of Radiology (research) and director of molecular and functional imaging at the H. Lee Moffitt Cancer Center and Research Institute, Tampa, FL.

A. Dean Sherry received a Ph.D. in Inorganic Chemistry from Kansas State University in 1967 and held a NIH postdoctoral fellowship before joining the chemistry faculty at the University of Texas at Dallas in 1972. He currently serves as Director of the Advanced Imaging Research Center on the campus of UT Southwestern Medical Center and holds academic appointments at UT Dallas (Chemistry) and UT Southwestern (Radiology). His research interests include metabolic imaging agents for MRI, ^{13}C hyperpolarization studies, and high-field MR imaging and spectroscopy.

REFERENCES

1 Caravan, P.; Ellison, J. J.; McMurray, T. J.; Lauffer, R. B. Gadolinium(III) Chelates as MRI Contrast Agents: Structure, Dynamics, and Applications. *Chem. Rev.* **1999**, *99*, 2293–2352.

2 Bellin, M. F. MR Contrast Agents, the Old and the New. *Eur. J. Radiol.* **2006**, *60*, 314–323.

3 Bellin, M. F.; Van Der Molen, A. J. Extracellular Gadolinium-Based Contrast Media: An Overview. *Eur. J. Radiol.* **2008**, *66*, 160–167.

4 Rooney, W. D.; Johnson, G.; Li, X.; Cohen, E. R.; Kim, S. G.; Ugurbil, K.; Springer, C. S., Jr. Magnetic Field and Tissue Dependencies of Human Brain Longitudinal ^1H_2O Relaxation in Vivo. *Magn. Reson. Med.* **2007**, *57*, 308–318.

5 Moats, R. A.; Fraser, S. E.; Meade, T. J. A "Smart" Magnetic Resonance Imaging Agent That Reports on Specific Enzymatic Activity. *Angew. Chem., Int. Ed. Engl.* **1997**, *36*, 726–728.

6 Louie, A. Y.; Huber, M. M.; Ahrens, E. T.; Rothbacher, U.; Moats, R.; Jacobs, R. E.; Fraser, S. E.; Meade, T. J. In Vivo Visualization of Gene Expression Using Magnetic Resonance Imaging. *Nat. Biotechnol.* **2000**, *18*, 321–325.

7 Perez, J. M.; O'Loughin, T.; Simeone, F. J.; Weissleder, R.; Josephson, L. DNA-Based Magnetic Nanoparticle Assembly Acts as a Magnetic Relaxation Nanoswitch Allowing Screening of DNA-Cleaving Agents. *J. Am. Chem. Soc.* **2002**, *124*, 2856–2857.

8 Atanasijevic, T.; Shusteff, M.; Fam, P.; Jasanoff, A. Calcium-Sensitive MRI Contrast Agents Based on Superparamagnetic Iron Oxide Nanoparticles and Calmodulin. *Proc. Natl. Acad. Sci. U.S.A.* **2006**, *103*, 14707–14712.

9 Taktak, S.; Sosnovik, D.; Cima, M. J.; Weissleder, R.; Josephson, L. Multiparameter Magnetic Relaxation Switch Assays. *Anal. Chem.* **2007**, *79*, 8863–8869.

10 Park, I.-K.; Ng, C.-P.; Wang, J.; Chu, B.; Yuan, C.; Zhang, S.; Pun, S. H. Determination of Nanoparticle Vehicle Unpackaging by MR Imaging of a T2 Magnetic Relaxation Switch. *Biomaterials* **2008**, *29*, 724–732.

11 Bulte, J. W. M.; Kraitchman, D. L. Iron Oxide MR Contrast Agents for Molecular and Cellular Imaging. *NMR Biomed.* **2004**, *17*, 484–499.

12 Hanaoka, K.; Lubag, A. J.; Castillo-Muzquiz, A.; Kodadek, T.; Sherry, A. D. The Detection Limit of a Gd^{3+}-Based T1 Agent Is Substantially Reduced When Targeted to a Protein Microdomain. *Magn. Reson. Imaging* **2008**, *26*, 608–617.

13 Jocher, C. J.; Botta, M.; Avedano, S.; Moore, E. G.; Xu, J.; Aime, S.; Raymond, K. N. Optimized Relaxivity and Stability of [Gd(H(2,2)-1,2-HOPO)(H_2O)]- as an MRI Contrast Agent. *Inorg. Chem.* **2007**, *46*, 4796–4798.

14 Udugamasooriya, D. G.; Dineen, S. P.; Brekken, R. A.; Kodadek, T. A Peptoid "Antibody Surrogate" That Antagonizes VEGF Receptor 2 Activity. *J. Am. Chem. Soc.* **2008**, *130*, 5744–5752.

15 Aime, S.; Botta, M.; Terreno, E. Gd(III)-based contrast agents for MRI. *Adv. Inorg. Chem.* **2006**, *57*, 173–237.

16 Lowe, M. P.; Parker, D.; Reany, O.; Aime, S.; Botta, M.; Castellano, G.; Gianolio, E.; Pagliarin, R. pH-Dependent Modulation of Relaxivity and Luminescence in Macrocyclic Gadolinium and Europium Complexes Based on Reversible Intramolecular Sulfonamide Ligation. *J. Am. Chem. Soc.* **2001**, *123*, 7601–7609.

17 Zhang, S.; Wu, K.; Dean Sherry, A. A Novel pH-Sensitive MRI Contrast Agent. *Angew. Chem., Int. Ed.* **1999**, *38*, 3192–3194.

18 Aime, S.; Botta, M.; Crich, S. G.; Giovenzana, G.; Palmisano, G.; Sisti, M. A Macromolecular Gd(III) Complex as pH-Responsive Relaxometric Probe for MRI Applications. *Chem. Commun.* **1999**, 1577–1578.

19 Ali, M. M.; Woods, M.; Caravan, P.; Opina, A. C.; Spiller, M.; Fettinger, J. C.; Sherry, A. D. Synthesis and Relaxometric Studies of a Dendrimer-Based pH-Responsive MRI Contrast Agent. *Chem.—Eur. J.* **2008**, *14*, 7250–7258.

20 Aime, S.; Fedeli, F.; Sanino, A.; Terreno, E. A R2/R1 Ratiometric Procedure for a Concentration-Independent, pH-Responsive, Gd(III)-Based MRI Agent. *J. Am. Chem. Soc.* **2006**, *128*, 11326–11327.

21 Raghunand, N.; Howison, C.; Sherry, A. D.; Zhang, S.; Gillies, R. J. Renal and Systemic pH Imaging by Contrast-Enhanced MRI. *Magn. Reson. Med.* **2003**, *49*, 249–257.

22 Raghunand, N.; Zhang, S.; Sherry, A. D.; Gillies, R. J. In Vivo Magnetic Resonance Imaging of Tissue pH Using a Novel pH-Sensitive Contrast Agent, GdDOTA-4AmP. *Acad. Radiol.* **2002**, *9*, S481–S483.

23 Garcia-Martin, M. L.; Martinez, G. V.; Raghunand, N.; Sherry, A. D.; Zhang, S.; Gillies, R. J. High Resolution pHe Imaging of Rat Glioma Using pH-Dependent Relaxivity. *Magn. Reson. Med.* **2006**, *55*, 309–315.

24 Chen, W.; Tomalia, D. A.; Thomas, J. L. Unusual pH-Dependent Polarity Changes in PAMAM Dendrimers: Evidence for pH-Responsive Conformational Changes. *Macromolecules* **2000**, *33*, 9169–9172.

25 Ward, K. M.; Aletras, A. H.; Balaban, R. S. A New Class of Contrast Agents for MRI Based on Proton Chemical Exchange Dependent Saturation Transfer (CEST). *J. Magn. Reson.* **2000**, *143*, 79–87.

26 Terreno, E.; Castelli, D. D.; Cravotto, G.; Milone, L.; Aime, S. Ln(III)-DOTAMGly Complexes: A Versatile Series to Assess the Determinants of the Efficacy of Paramagnetic Chemical Exchange Saturation Transfer Agents for Magnetic Resonance Imaging Applications. *Invest. Radiol.* **2004**, *39*, 235–243.

27 Sherry, A. D.; Woods, M. Chemical Exchange Saturation Transfer Contrast Agents for Magnetic Resonance Imaging. *Annu. Rev. Biomed. Eng.* **2008**, *10*, 391–411.

28 McMahon, M. T.; Gilad, A. A.; Zhou, J.; Sun, P. Z.; Bulte, J. W. M.; Van Zijl, P. C. M. Quantifying Exchange Rates in Chemical Exchange Saturation Transfer Agents Using the Saturation Time and Saturation Power Dependencies of the Magnetization Transfer Effect on the Magnetic Resonance Imaging Signal: pH Calibration for Poly-L-lysine and a Starburst Dendrimer. *Magn. Reson. Med.* **2006**, *55*, 836–847.

29 Zhou, J.; Payen, J. F.; Wilson, D. A.; Traystman, R. J.; Van Zijl, P. C. M. Using the Amide Proton Signals of Intracellular Proteins and Peptides To Detect pH Effects in MRI. *Nat. Med.* **2003**, *9*, 1085–1090.

30 Zhou, J.; Van Zijl, P. C. M. Chemical Exchange Saturation Transfer Imaging and Spectroscopy. *Prog. Nucl. Magn. Reson. Spectrosc.* **2006**, *48*, 109–136.

31 Zhang, S.; Malloy, C. R.; Sherry, A. D. MRI Thermometry Based on PARACEST Agents. *J. Am. Chem. Soc.* **2005**, *127*, 17572–17573.

32 Trokowski, R.; Zhang, S.; Sherry, A. D. Cyclen-Based Phenylboronate Ligands and Their Eu^{3+} Complexes for Sensing Glucose by MRI. *Bioconjug. Chem.* **2004**, *15*, 1431–1440.

33 Ren, J.; Trokowski, R.; Zhang, S.; Malloy, C. R.; Sherry, A. D. Imaging the Tissue Distribution of Glucose in Livers Using a PARACEST Sensor. *Magn. Reson. Med.* **2008**, *60*, 1047–1055.

34 Pikkemaat, J. A.; Wegh, R. T.; Lamerichs, R.; van de Molengraaf, R. A.; Langereis, S.; Burdinski, D.; Raymond, A. Y. F.; Janssen, H. M.; de Waal, B. F. M.; Willard, N. P.; Meijer, E. W.; Grüll, H. Dendritic PARACEST Contrast Agents for Magnetic Resonance Imaging. *Contrast Media Mol. Imaging* **2007**, *2*, 229–239.

35 Wegh, R. T.; Pikkemaat, J. A.; Willard, N. P. Method for using CEST contrast agents in MRI, World Patent WO IB51237, 2006114739, 2006.